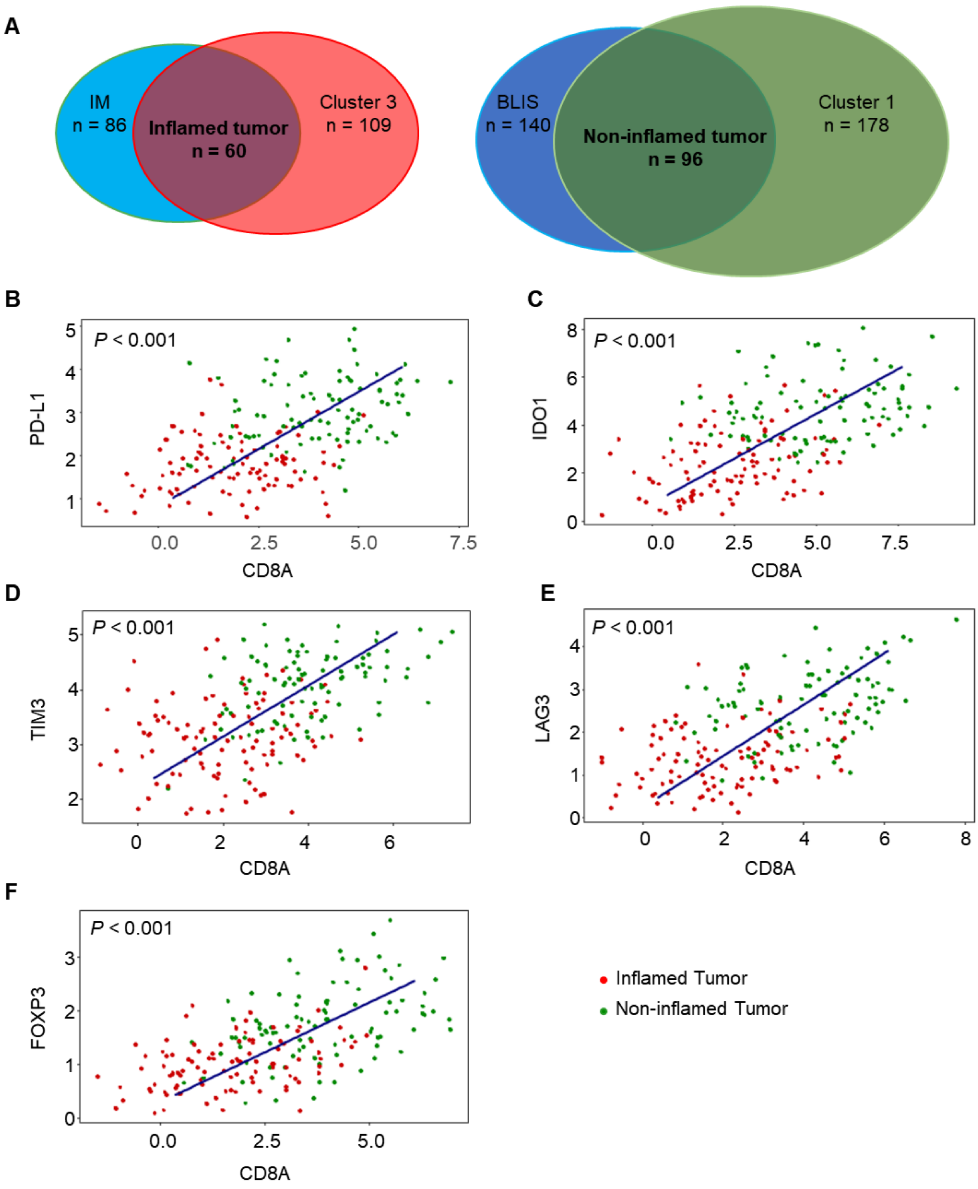

Supplemental Figure S1. Definition and characteristics of two distinct microenvironmental subtypes in our study.

(A) Definition of the "Inflamed tumor" (IM & cluster 3) and "non-inflamed tumor" (BLIS & cluster 1) immune microenvironment in our study. **(B)** Positive correlation between the expression of *PD-L1* and that of *CD8A* ($P < 0.001$, Pearson correlation). Inflamed tumors (red) show higher expression of both genes than non-inflamed tumors (blue). **(C-F)** The additional immune-inhibitory molecules, *IDO1* (C), *TIM3* (D), *LAG3* (E) and *FOXP3* (F), showing similar significant correlations (all $P < 0.001$, Pearson correlation). IM, immunomodulatory; BLIS, basal-like immune-suppressed.

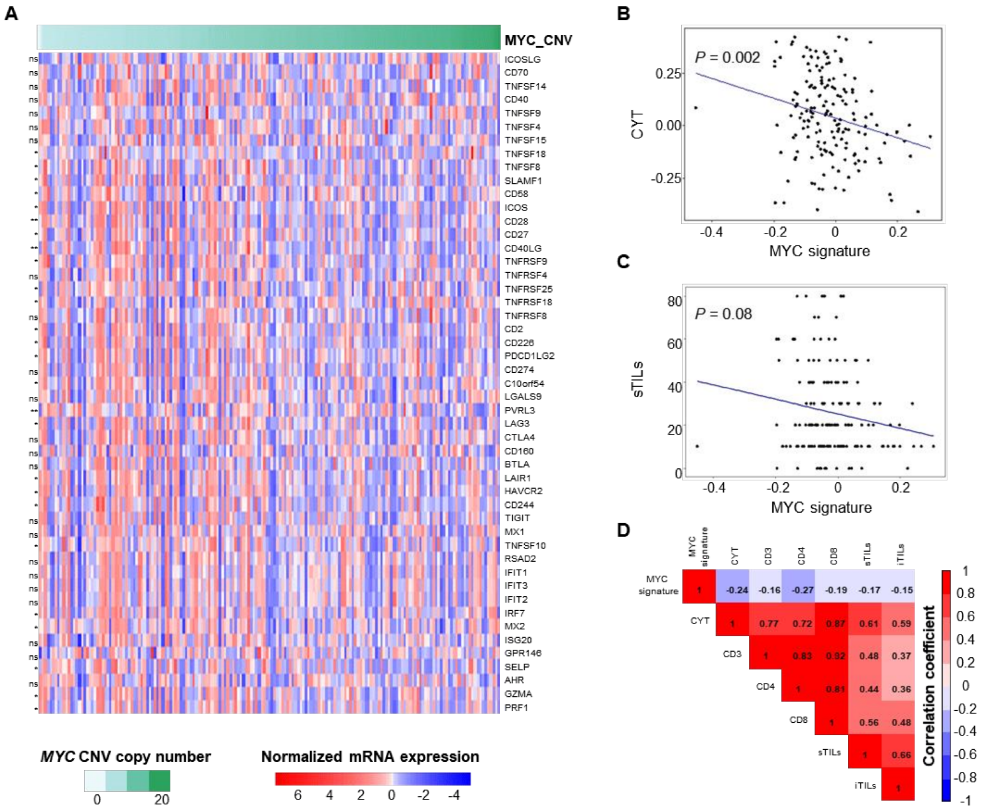

Supplemental Figure S2. Correlations between *MYC* amplification, expression and immune-related indicators.

(A) Heatmap showing the relationship between *MYC* CNV levels and immune-related genes. **(B-C)** Correlations of the CYT (B), sTILs (C) and MYC transcriptional signature in TNBC patients from the FUSCC cohort. **(D)** Heatmap correlation matrix of the association of the MYC transcriptional signature and classic IHC markers in TNBC. CNV, copy number variation; CYT, cytolytic activity; sTILs, stromal tumor-infiltrating lymphocytes. Pearson correlation was used to assess the relationship between two indicators.

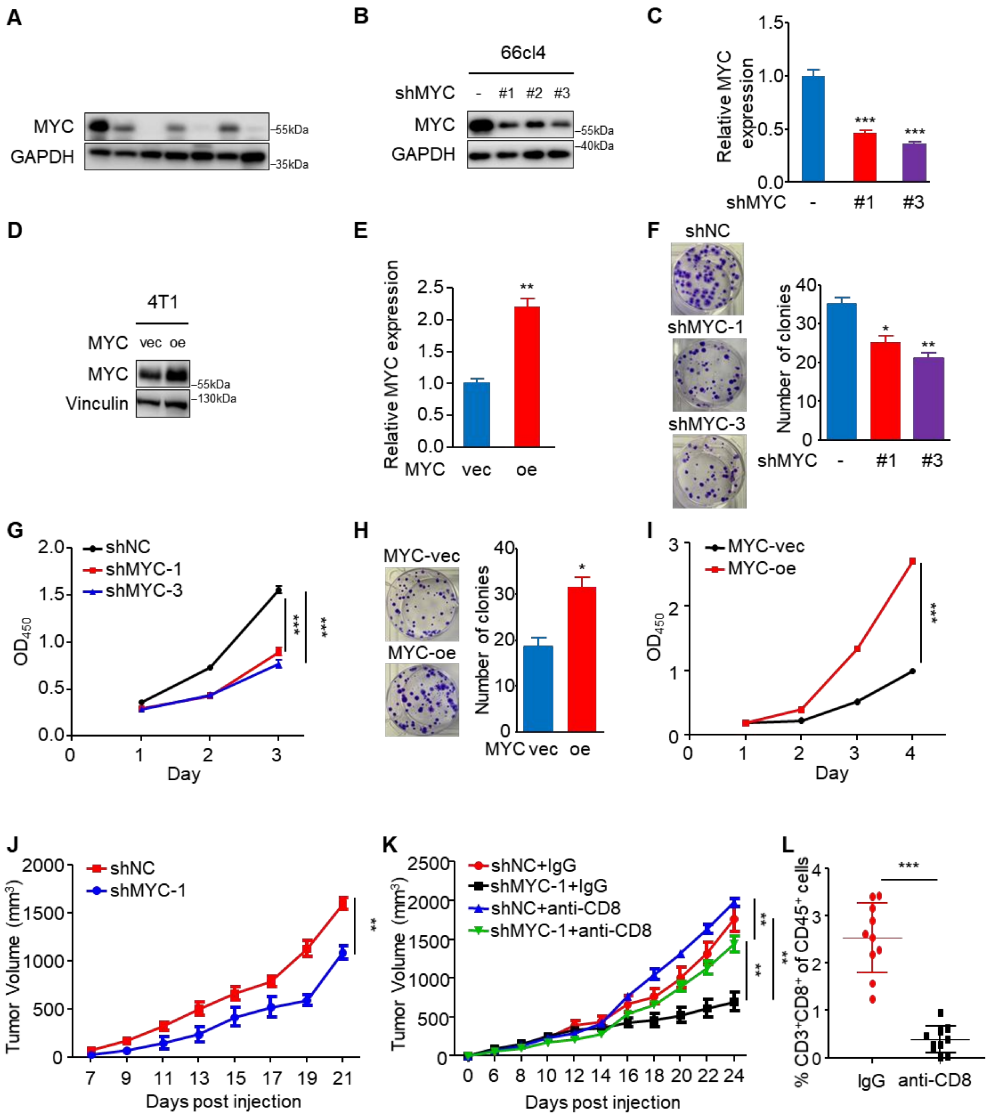

Supplemental Figure S3. The effects of MYC knockdown and overexpression on cell proliferation and tumor growth.

(A) Immunoblotting analyses of MYC in murine cell lines (67NR, 66cl4, TS/A, 4T1, 4T07, 4T1.2, 168FARN). **(B-C)** Immunoblotting (B) and RT-qPCR (C) analyses to confirm MYC knockdown at the protein and mRNA levels in 66cl4 cells. **(D-E)** Immunoblotting (D) and RT-qPCR (E) analyses to confirm MYC overexpression at the mRNA and protein levels in 4T1 cells. **(F)** Representative images of surviving colonies with 66cl4 cells expressing shNC/MYC and the corresponding quantitative results. **(G)** *In vitro* growth curves of 66cl4 cells evaluated by a CCK-8 assay. **(H)** Representative images of surviving colonies with 4T1 cells expressing MYC-vec/oe and the corresponding quantitative results. **(I)** *In vitro* growth curves of 4T1 cells evaluated by a CCK-8 assay. **(J)** Tumor volumes of 66cl4-shNC and 66cl4-shMYC subcutaneous tumors in NSG mice (21 days; n = 5), as measured using calipers. **(K)** Tumor volumes of 66cl4-shNC and 66cl4-shMYC subcutaneous tumors

in BALB/c mice (24 days; n = 5) treated with rat IgG or CD8-depleting antibody, as measured using calipers. **(L)** Percentage of $CD3^+CD8^+$ T cells in $CD45^+$ cells in the blood from mice treated with rat IgG or CD8-depleting antibody (n = 10 mice per group) as measured by flow cytometry. The data are presented as the mean ± SEM (C, E, F, G, H, I, J, K and L); two-tailed unpaired Student's t test (C, E, F, H and L); one-way ANOVA test after adjusting for multiple comparisons (G, I, J and K). **P* < 0.05; ***P* < 0.01; ****P* < 0.001. ANOVA, analysis of variance; RT-qPCR, quantitative reverse transcription PCR; SEM, standard error of mean.

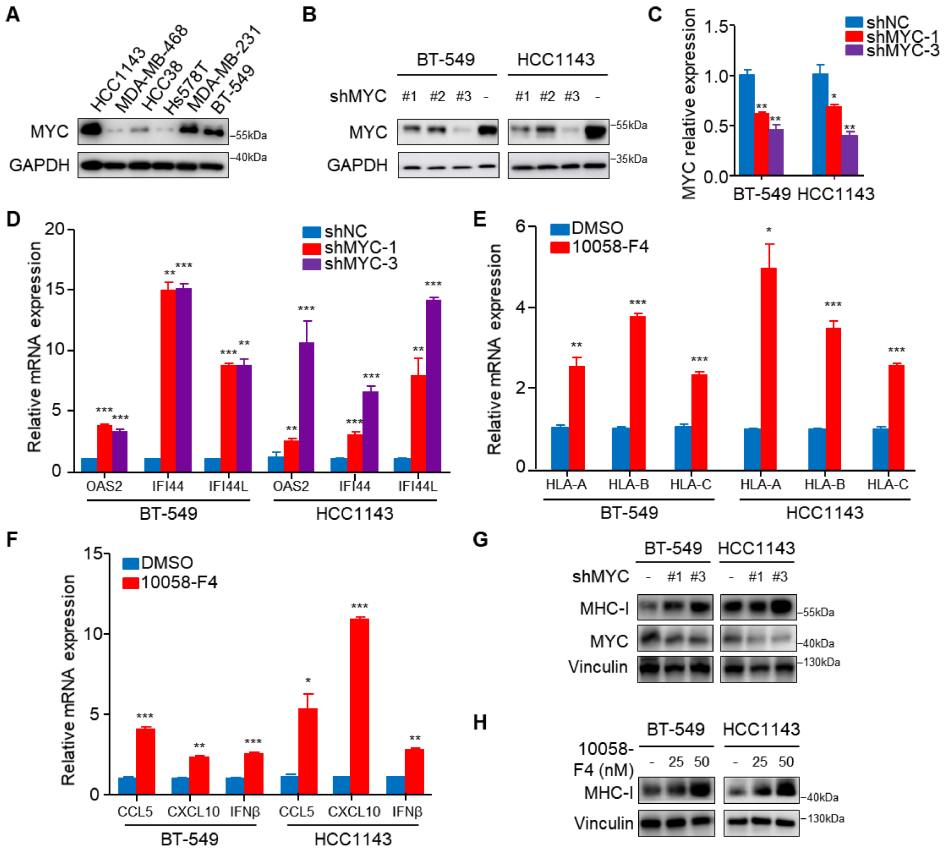

Supplemental Figure S4. MYC knockdown verification, and analyses of interferon downstream gene expressions after MYC knockdown or treatment with 10058-F4 in human TNBC cell lines. **(A)** Immunoblotting analyses of MYC in human TNBC cell lines (HCC1143, MDA-MB-468, HCC38, Hs578T, MDA-MB-231, and BT-549). **(B-C)** Immunoblotting (B) and RT-qPCR (C) analyses to confirm MYC knockdown at the mRNA and protein levels in BT-549 and HCC1143 cells. **(D)** RT-qPCR analyses of the mRNA expression of ISGs including OAS2, IFI44, and IFI44L in BT-549 and HCC1134 cells with MYC knockdown. **(E)** RT-qPCR analyses of MHC-I mRNA expression in BT-549 and HCC1143 cells after treatment with DMSO or 10058-F4 (25 nM or 50 nM). **(F)** RT-qPCR analyses of CCL5, CXCL10 and IFNβ mRNA expression in BT-549 and HCC1134 cells after treatment with DMSO or 10058-F4 (25 nM or 50 nM). **(G-H)** Immunoblotting analyses of MHC-I expression in BT-549 and HCC1134 cells after MYC knockdown (G) and treatment with DMSO or 10058-F4 (25 nM or 50 nM) (H). The data are presented as the mean ± SEM (C, D, E and F); n = 3 independent experiments (C, D, E and F); two-tailed unpaired Student's t test (C, D, E and F). *P < 0.05; **P < 0.01; ***P < 0.001. ISG, IFN-stimulated gene; IFNβ, interferon β; RT-qPCR, quantitative reverse transcription PCR; SEM, standard error of mean.

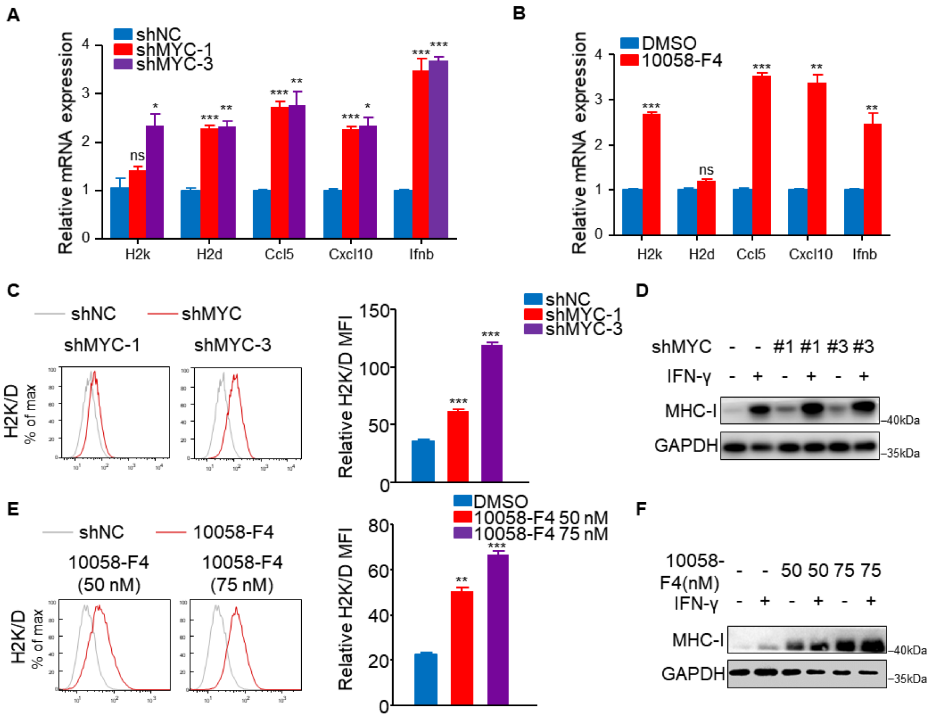

Supplemental Figure S5. Analyses of interferon downstream gene expressions after MYC knockdown or treatment with 10058-F4 in 66cl4 cells.

(A-B) RT-qPCR analyses of MHC-I, Ccl5, Cxcl10, and Ifnb mRNA expression in 66cl4 cells with MYC knockdown (A) or after treatment with DMSO or 10058-F4 (75nM) (B). **(C-D)** Flow cytometry (C) and immunoblotting (D) analyses of MHC-I expression in 66cl4 cells after MYC knockdown with/without IFN-γ. **(E-F)** Flow cytometry (E) and immunoblotting (F) analyses of MHC-I expression in 66cl4 cells with MYC treated with DMSO or 10058-F4 (50 nM or 75 nM) with/without IFN-γ. The data are presented as the mean ± SEM (A, B, C and E); n = 3 independent experiments (A, B, C and E); two-tailed unpaired Student's t test (A, B, C and E). *$P < 0.05$; **$P < 0.01$; ***$P < 0.001$; ns, not significant. RT-qPCR, quantitative reverse transcription PCR; SEM, standard error of mean.

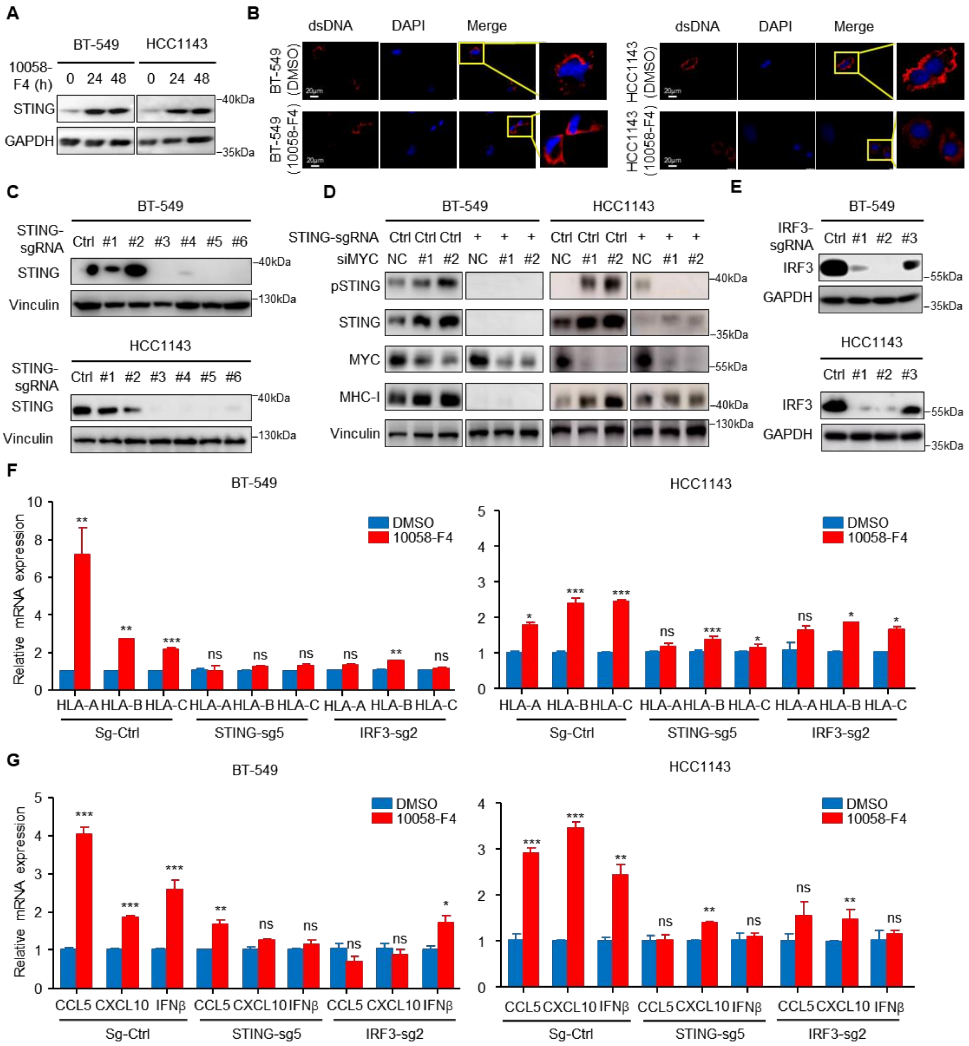

Supplemental Figure S6. 10058-F4-induced increase in interferon downstream gene expressions is dependent on cGAS-STING pathway.

(A) Immunoblotting analyses of STING expression in BT-549 and HCC1143 cells after treatment with DMSO or 10058-F4 (24 and 48 h). **(B)** dsDNA and DAPI staining of BT-549 and HCC1143 cells using immunofluorescence after treatment with DMSO or 10058-F4 (50 nM). **(C)** Immunoblotting analyses to measure STING knockdown at the protein levels in BT-549 (left) and HCC1143 (right) cells. **(D)** Immunoblotting analyses to measure STING activation [phospho STING (S366)] in BT-549 and HCC1143 cells transfected with MYC-siRNAs or NC-siRNA in the negative control and STING-knockdown groups. **(E)** Immunoblotting analyses to measure IRF3 knockdown at the protein levels in BT-549 (left) and HCC1143 (right) cells. **(F)** RT-qPCR analyses of HLA/A/B/C mRNA expression in BT-549 (left) and HCC1134 (right) cells after treatment with DMSO or 10058-F4 in the negative control, STING- and IRF3-knockdown groups. **(G)** RT-qPCR analyses of CCL5, CXCL10 and IFNβ mRNA expression in BT-549 (left) and HCC1134 (right) cells after treatment with DMSO or 10058-F4 in the negative control, STING- and IRF3-knockdown groups.The data are presented as the

mean ± SEM (F and G); n = 3 independent experiments (F and G); two-tailed unpaired Student's t test (F and G). **P* < 0.05; ***P* < 0.01; ****P* < 0.001; ns, not significant. DAPI, 2-(4-Amidinophenyl)-6-indolecarbamidine; IFNβ, interferon β; RT-qPCR, quantitative reverse transcription PCR; SEM, standard error of mean.

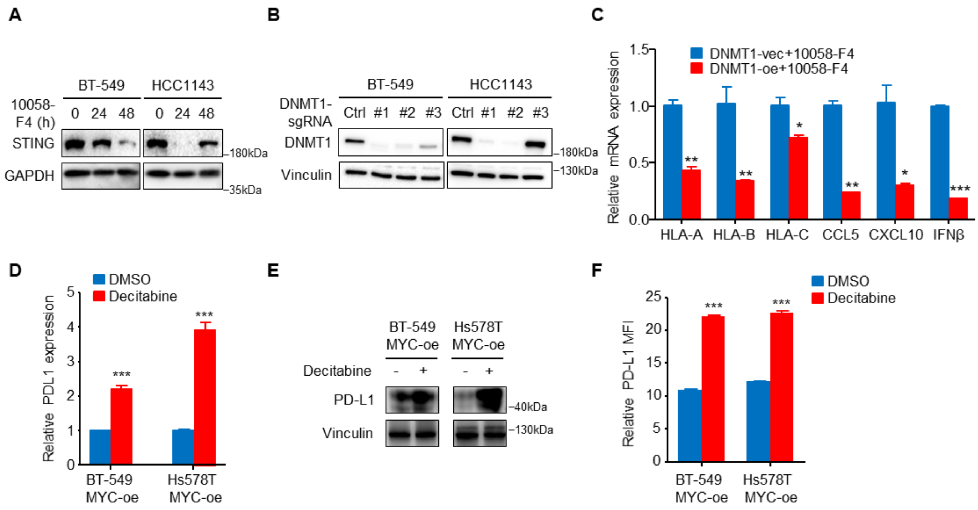

Supplemental Figure S7. 10058-F4-induced decrease in DNMT1 expression, DNMT1 knockdown verification, and decitabine-induced enhancement in PD-L1 expression, measured by immunoblotting.

(A) Immunoblotting analyses of DNMT1 expression in BT-549 and HCC1143 cells after treatment with DMSO or 10058-F4 (24 h and 48 h). **(B)** Effect of DNMT1 overexpression on downsteam gene expression in BT-549 cells after treatment with 10058-F4. **(C)** Immunoblotting analyses to measure DNMT1 knockdown in protein levels in BT-549 (left) and HCC1143 (right) cells. **(D-F)** RT-qPCR (D), immunoblotting (E) and flow cytometry (F) analyses of PD-L1 expression in MYC-overexpressing BT-549 and Hs578T cells treated with DMSO or decitabine. The data are presented as the mean ± SEM (C, D and F); n = 3 independent experiments (C, D and F); two-tailed unpaired Student's t test (C, D and F). **P* < 0.05; ***P* < 0.01; ****P* < 0.001. IFNβ, interferon β; RT-qPCR, quantitative reverse transcription PCR; SEM, standard error of mean.

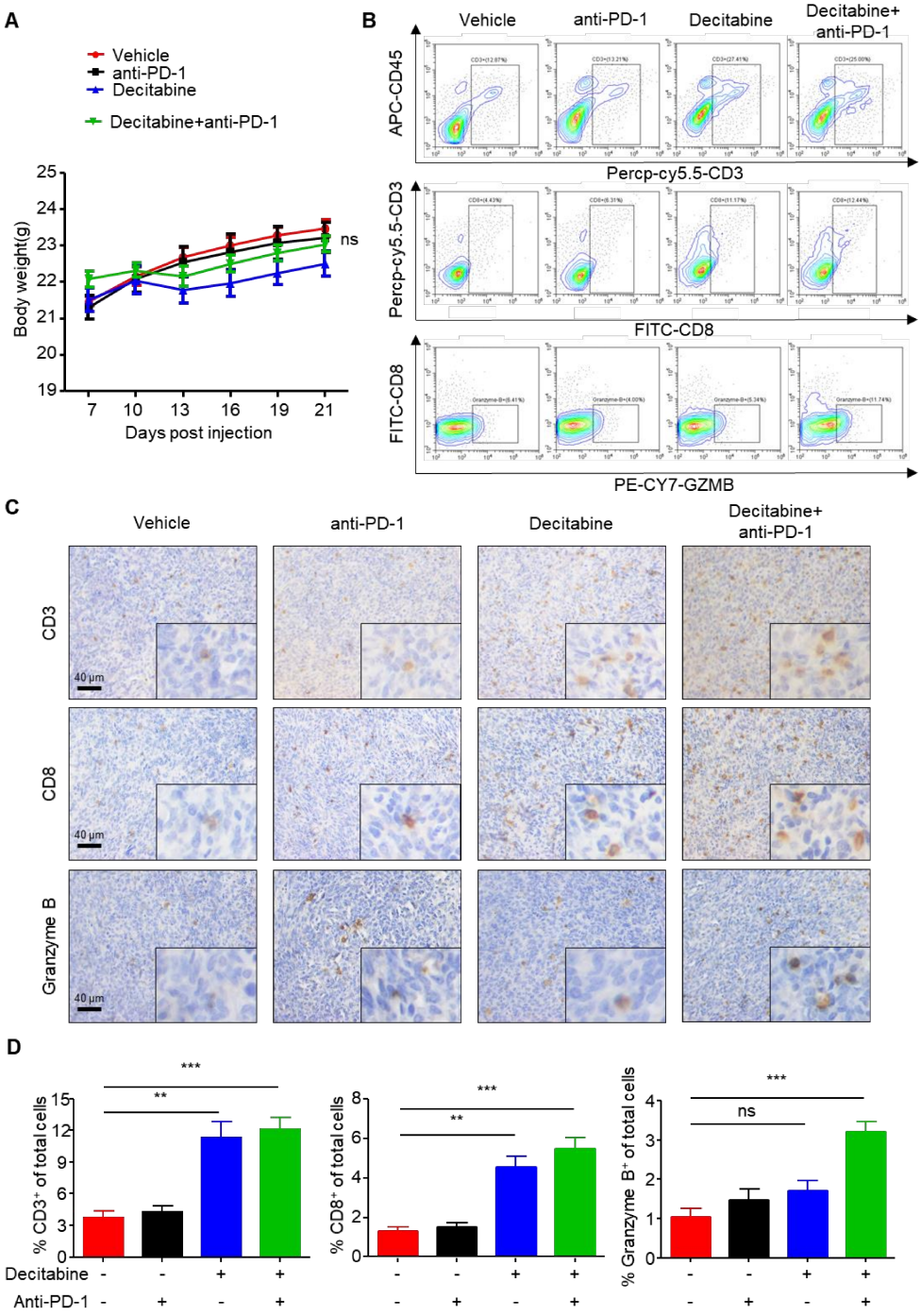

Supplemental Figure S8. Analyses of drug toxicity, and immune infiltrates of tumors in the four treatment groups.

(A) Mice body weight changes during the treatment period. **(B)** Representative flow cytometry analyses of $CD3^+$, $CD8^+$ and $CD8^+$Granzyme B^+ cells in the total live cell population in the four treatment groups. **(C)** Representative images of IHC for CD3, CD8 and Granzyme B in subcutaneous

tumors in the four treatment groups. **(D)** Quantification of $CD3^+$, $CD8^+$ and granzyme B^+ IHC performed on subcutaneous tumors in the four treatment groups. The data are presented as the mean ± SEM (A and D); n = 7 mice/group; two-tailed unpaired Student's t test (A and D). $^{**}P < 0.01$; $^{***}P < 0.001$; ns, not significant. SEM, standard error of mean.

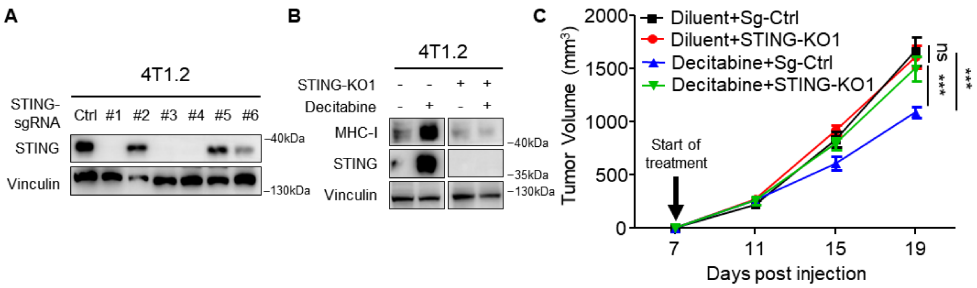

Supplemental Figure S9. Decitabine's antitumor efficacy is dependent on the tumor-expressed STING.

(A) Immunoblotting analyses to measure STING knockdown in protein levels in 4T1.2 murine cell line. **(B)** Immunoblotting analyses to measure STING and downsteam MHC-I expression in 4T1.2 cell in the negative control and STING-knockdown groups. **(C)** Tumor volumes of 4T1.2 negative control (Sg-Ctrl) and STING-knockdown (STING-KO1) subcutaneous tumors in BALB/c mice treated with diluent or decitabine. The data are presented as the mean ± SEM (C); one-way ANOVA test after adjusting for multiple comparisons (C). ***$P < 0.001$; ns, not significant. ANOVA, analysis of variance; SEM, standard error of mean.